This pdf file consists of figures containing photographs, and their captions, scanned from:

DYNAMIC GRAIN BOUNDARY MIGRATION AND FABRIC DEVELOPMENT: OBSERVATIONS, EXPERIMENTS AND SIMULATIONS

by

Mark Walter Jessell

A Dissertation

Submitted to the State University of New York at Albany

in Partial Fulfillment of

the Requirements for the Degree of

Doctor of Philosophy

College of Sciences and Mathematics

Department of Geological Sciences

1986

a

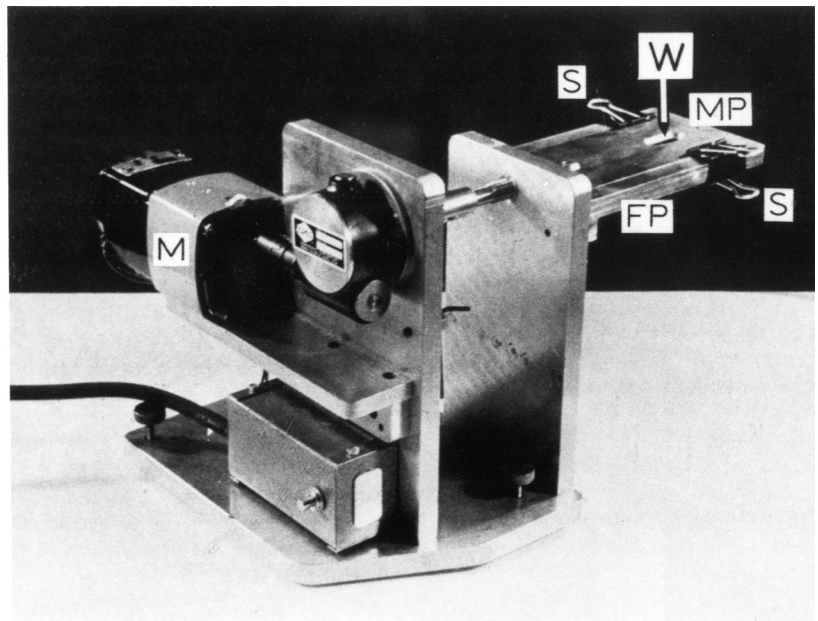

b

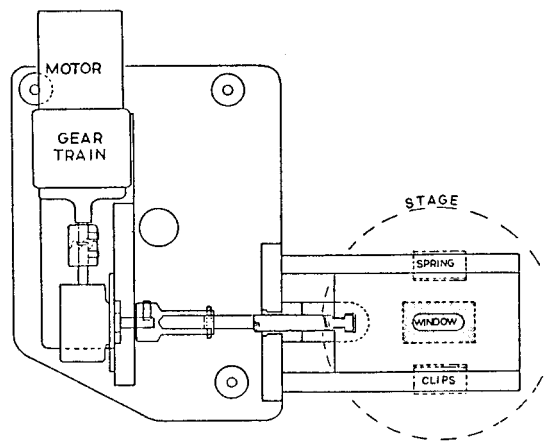

Fig.2.1 Hajeck apparatus. a) Photograph of apparatus, showing : motor and gear train (M); window (W); fixed plate holding lower glass (FP); moving plate holding upper slide (MP); and spring clips (S) After Means & Xia 1981 b) Plan view of Hajeck apparatus.

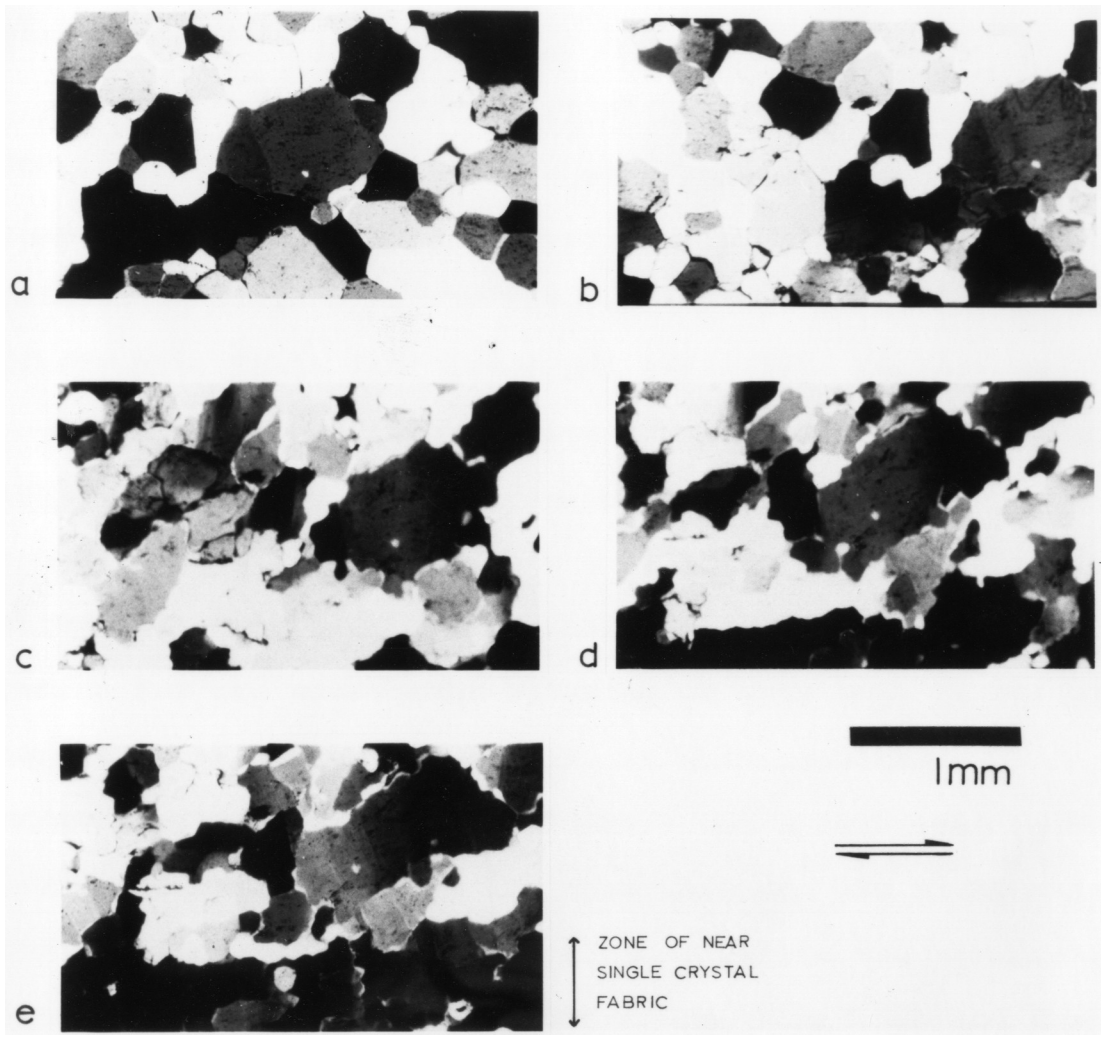

Fig.2.3 Photographic record of experiment TO-47, with photographs taken after a) 0 hours, b) 1 hours, c) 3 hours, d) 5 hours and e) 6 hours. Note the formation of a band of dark grains at the bottom of the photograph. Crossed nicols parallel to the photograph edges.

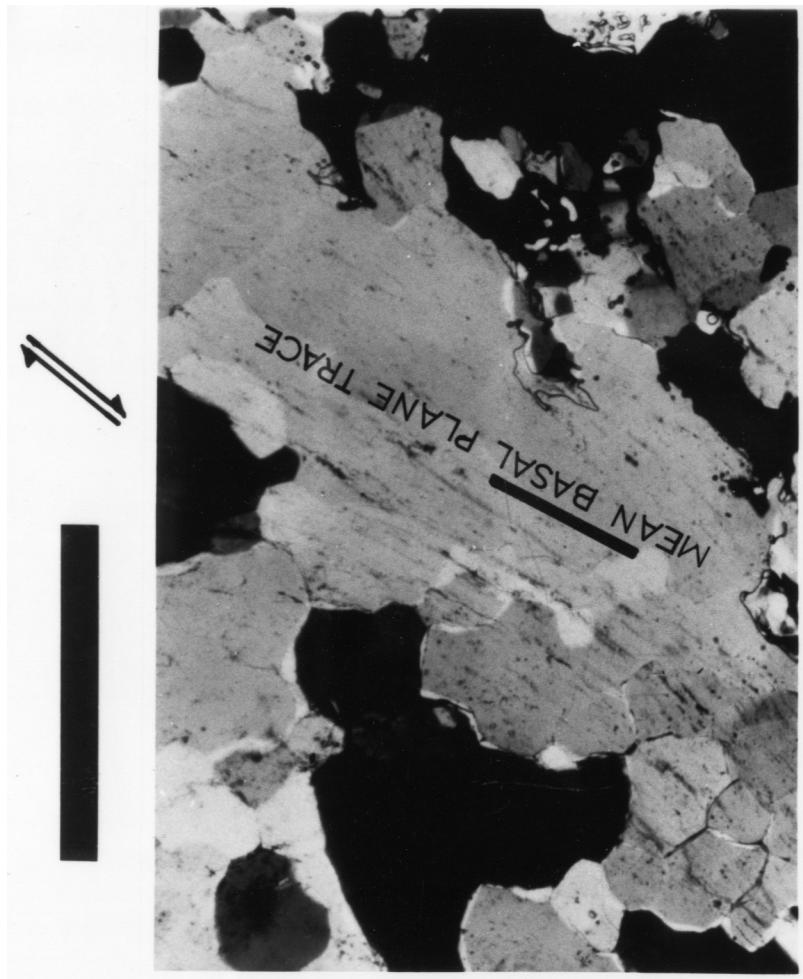

Fig.2.4 Near single crystal fabric developed during unobserved portion of the experiment, presumably by widening of the band seen in Fig.2.3. Crossed nicols parallel to the photograph edges. Scale bar represents 1 mm.

Fig.2.6 Experiment TO-55 a) Grain boundary in undeformed state, with marker particles circled. b) Grain boundary in deformed state. c) Map of area in deformed state. Solid line marks the old position of the grain boundary, and the dotted line marks the new position of the grain boundary. Vectors represent displacement vectors for individual particles (arrow heads mark new position) which indicate dextral simple shear with a component of sinistral shear at or near the grain boundary. The short bars show the orientation of the maximum stretch (S_1) for each grain. Scale bar represents 0.1 mm .

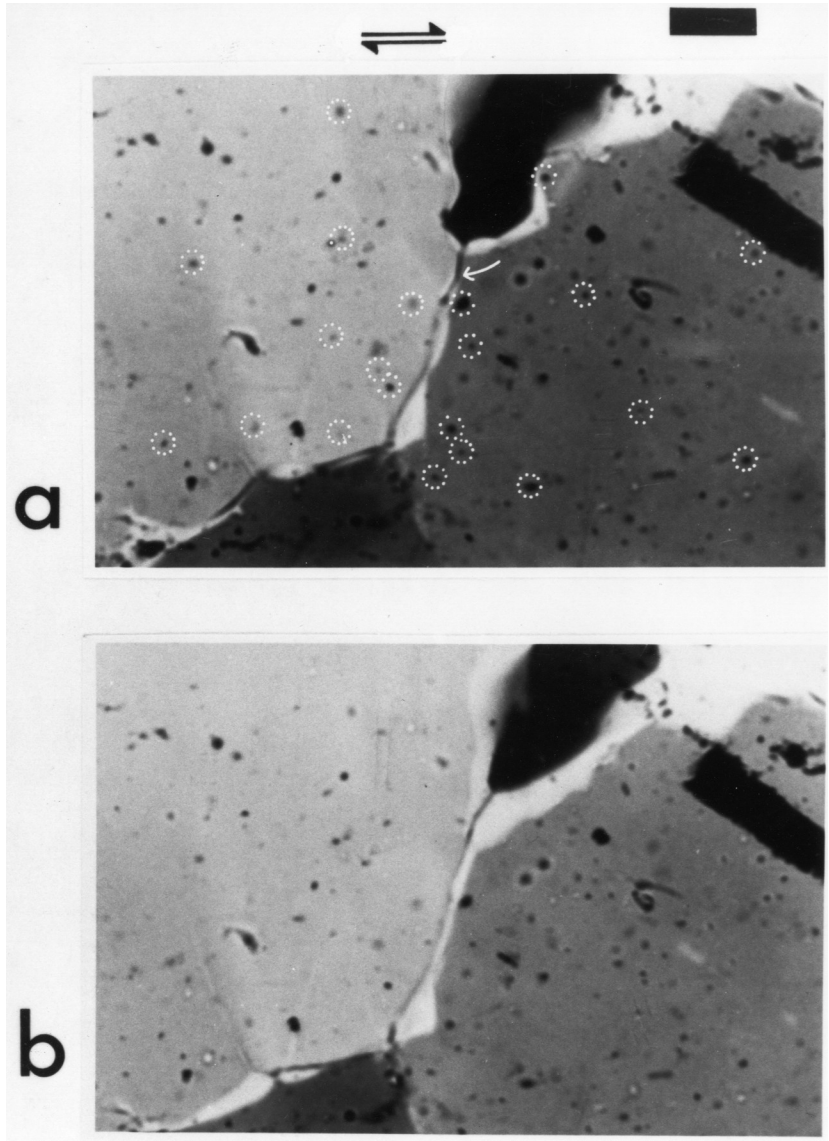
a
b

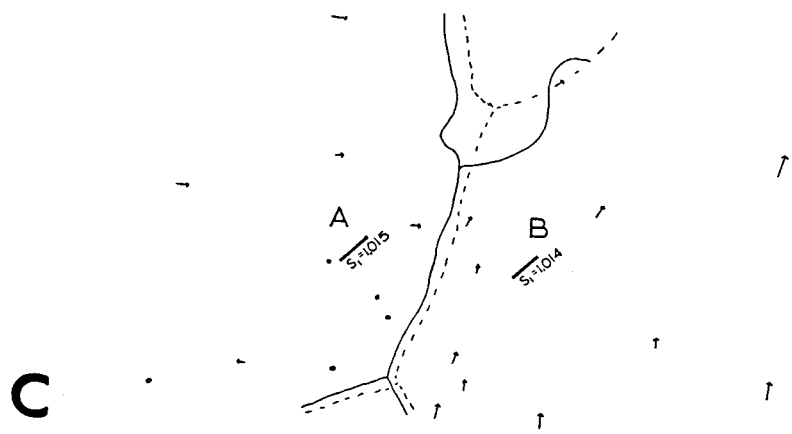
A
S1=1.015
B
S1=1.014
c

Fig.2.10 Photographic record of experiment TO-63, taken at cummulative deformation times of a) 0 hours, b) 2 hours, c) 4 hours, d) 6 hours, e) 8 hours and f) 8 hours (after 10 hours of static recovery). Stars show the position of specific marker particles. The obliquity of the grain shape foliation and the orientation of maximum finite elongation is demonstrated in 2.10.e.

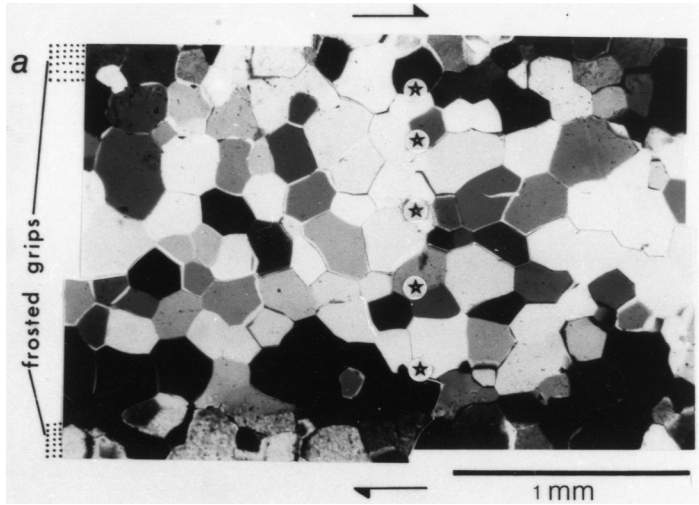
a
frosted grips
1 mm

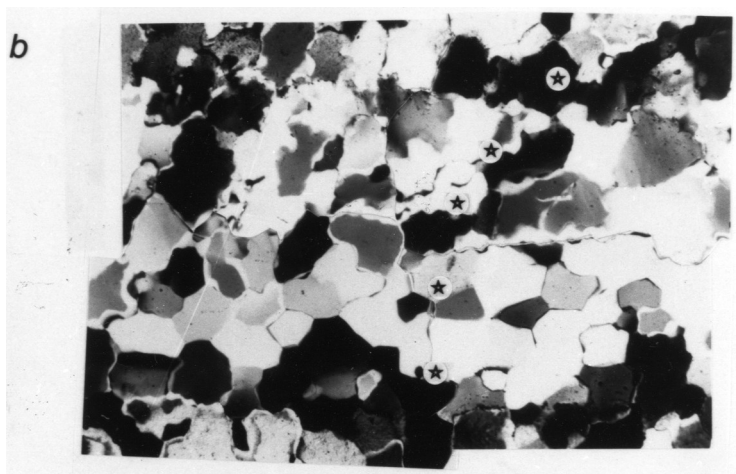
b

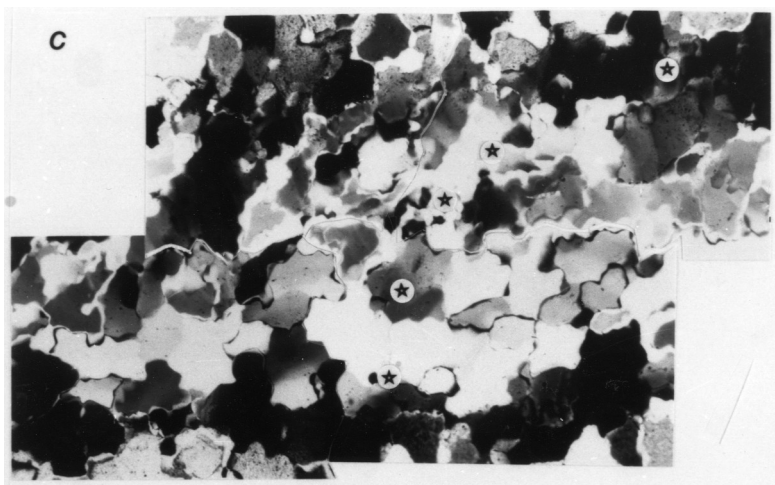
c

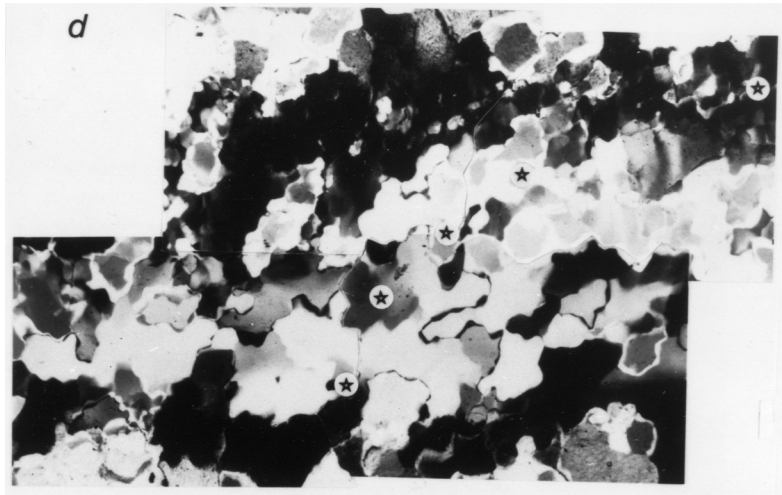
d

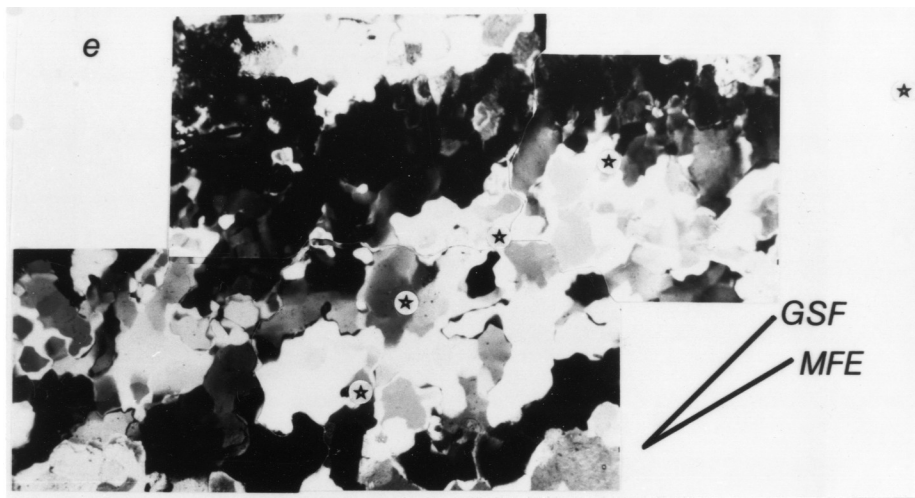
e
GSF
MFE

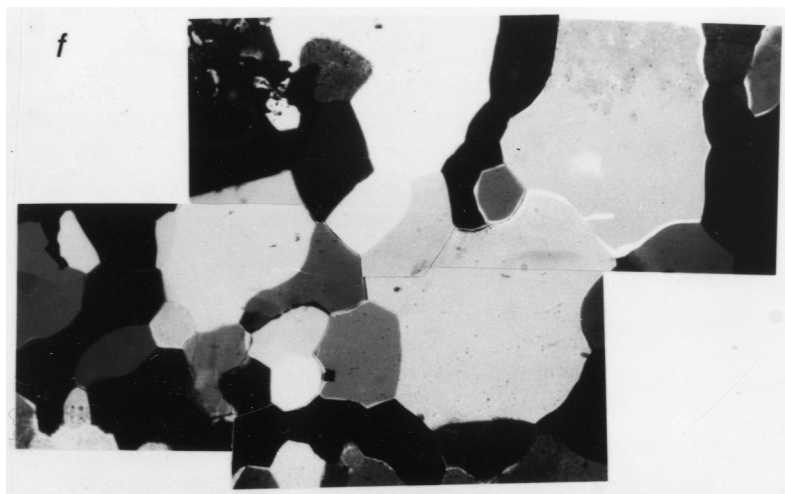
f

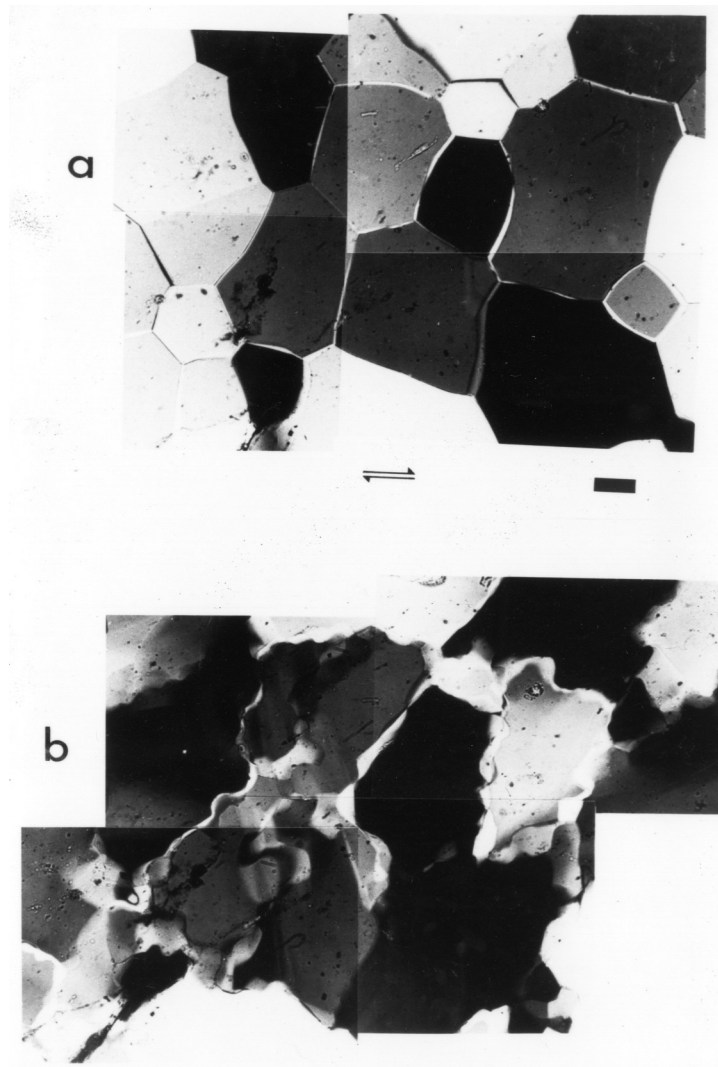

Fig.2.17 Photographic record of experiment TO-64, a) in the undeformed state, b) after 2 hours. Scale bar represents 0.1 mm.

Fig.2.18 Photographic record of experiment TO-65, a) in the undeformed state, b) after 1 hour, c) after 2 hours. Scale bar represents 0.1 mm. Marker particles show up clearly as black specks in these photographs.

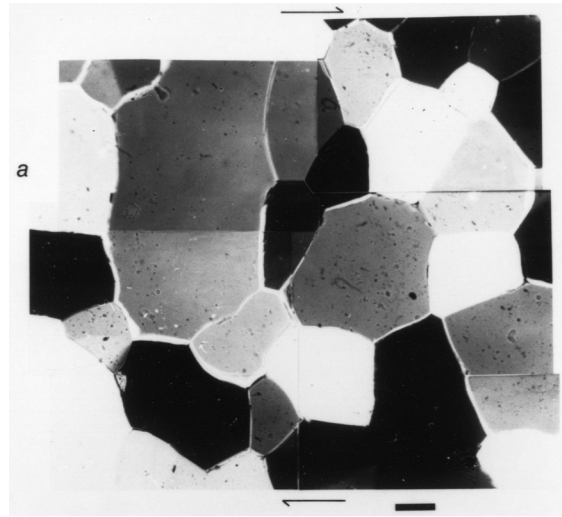
a

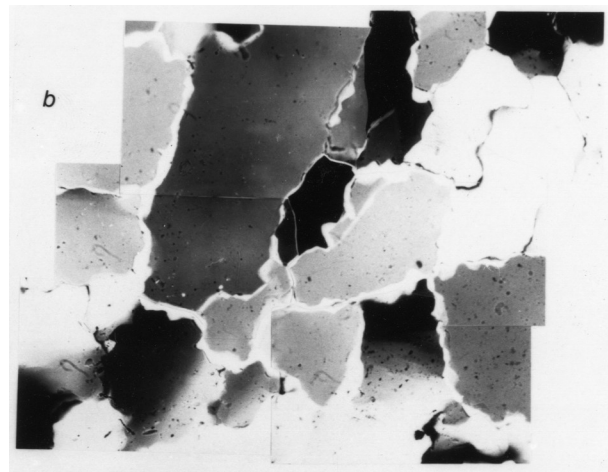
b

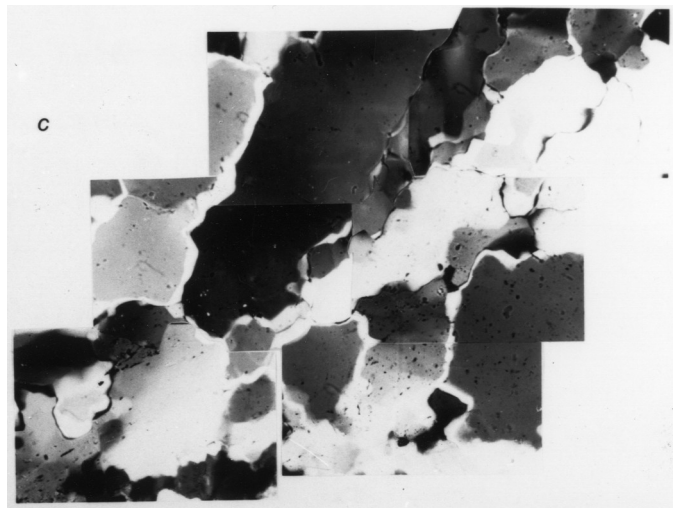
c

Fig.2.26 Photographic record of experiment TO-69. a) Grain boundary (single arrow) and subgrain boundary (double arrow), in the undeformed state. Star is a reference marker particle. b) Migrated boundaries after rapid small increment of dextral simple shear parallel to long axis of photograph. Arrow points to a newly formed subgrain. c) Migrated boundaries after rapid small increment of sinistral simple shear parallel to long axis of photograph. Grain boundary has continued to migrate in the same direction, whereas the subgrain boundary has reversed its migration direction. Scale bar represents 0.1 mm.

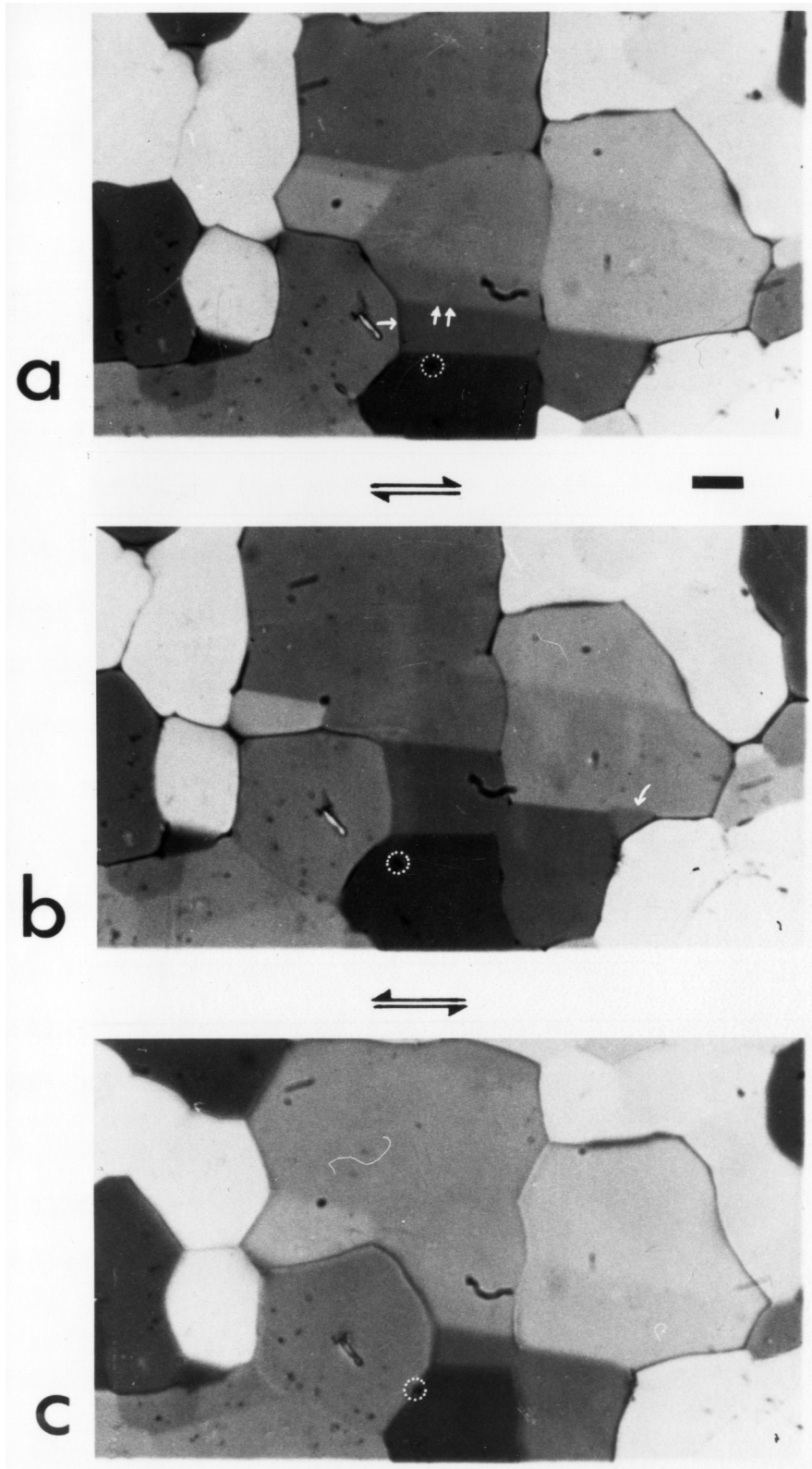
a
b
c

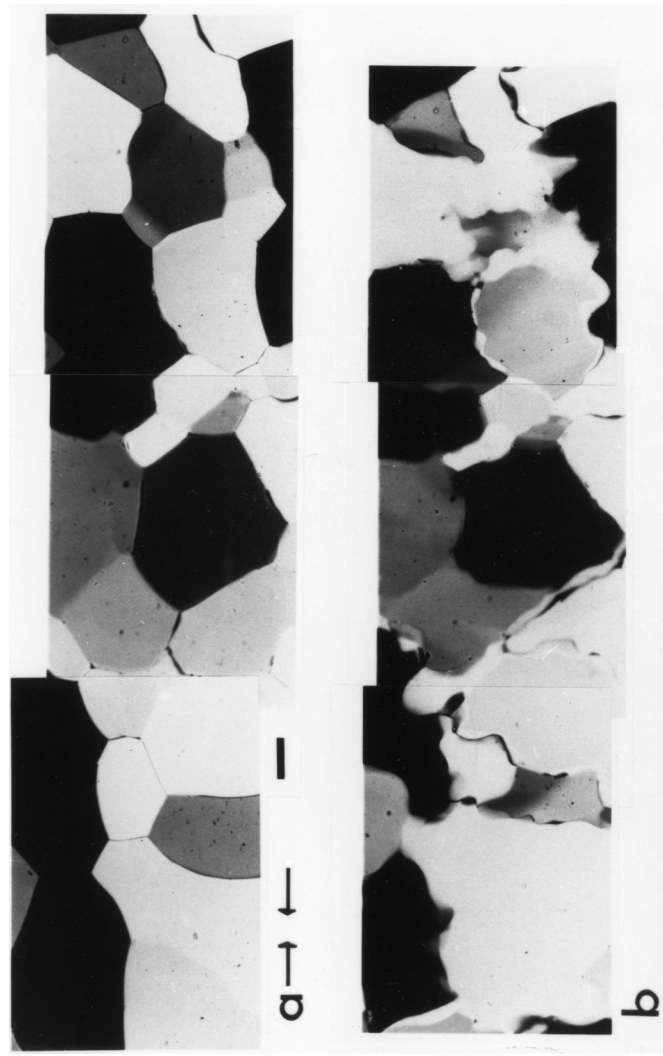

Fig.2.27 Photographic record of experiment TO-77, with photographs taken after a) 0 hours and b) 3 hours. Scale bar represents 0.1 mm.

Fig.3.1. a) Photo-micrographs in plane and polarised light of quartzite, slide cut perpendicular to foliation and to lineation, showing anastamosing nature of muscovite films. b) Photomicro-graphs in plane and polarised light of quartzite cut perpendicular to foliation and parallel to lineation.

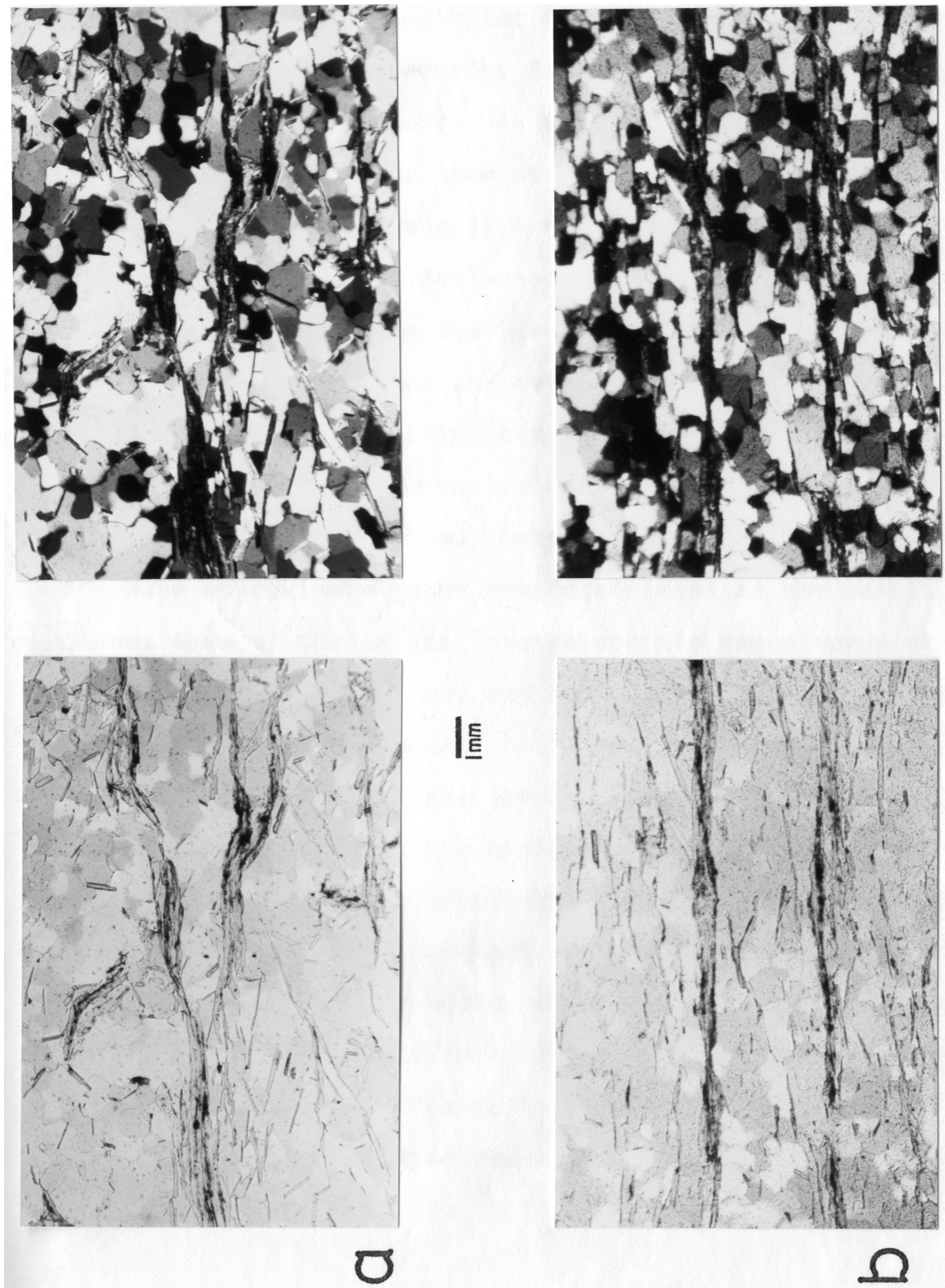
1mm
a
b

Fig.3.3. a) Photo-micrograph of "pinning" micro-stucture. b) Postulated mode of formation of "pinning" microstructure. A and B are quartz grains, the black grain is a mica. c) Alternative hypothesis to explain "pinning" microstructure. Cross-hatched area represents area of damaged quartz lattice around mica grain, which is preferentially consumed by grain B.

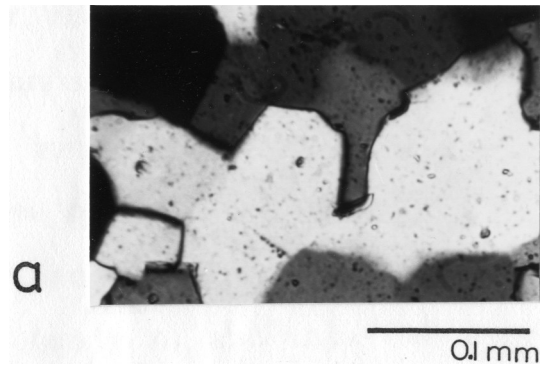
a
0.1 mm

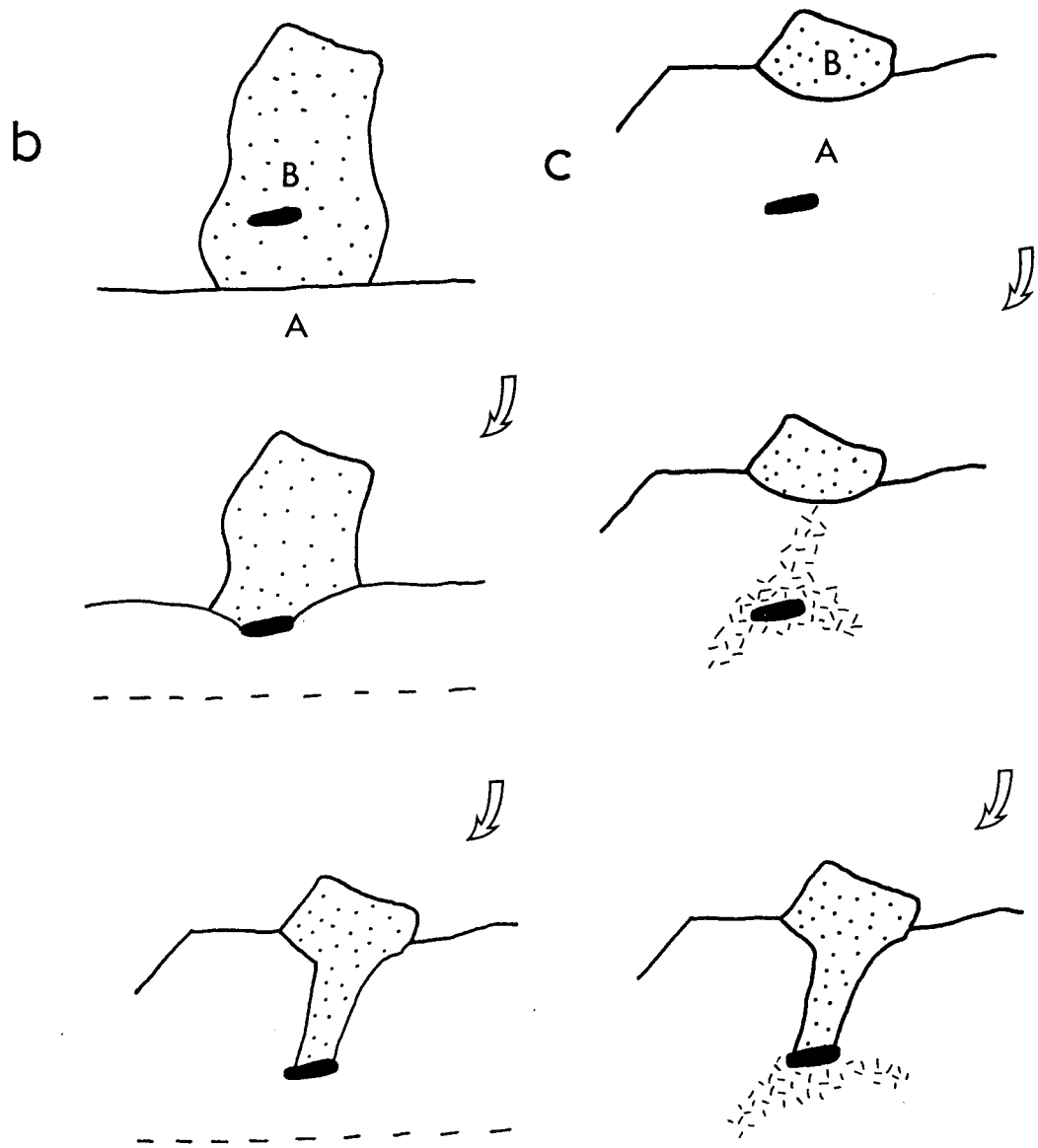
b
B
A
c
B
A

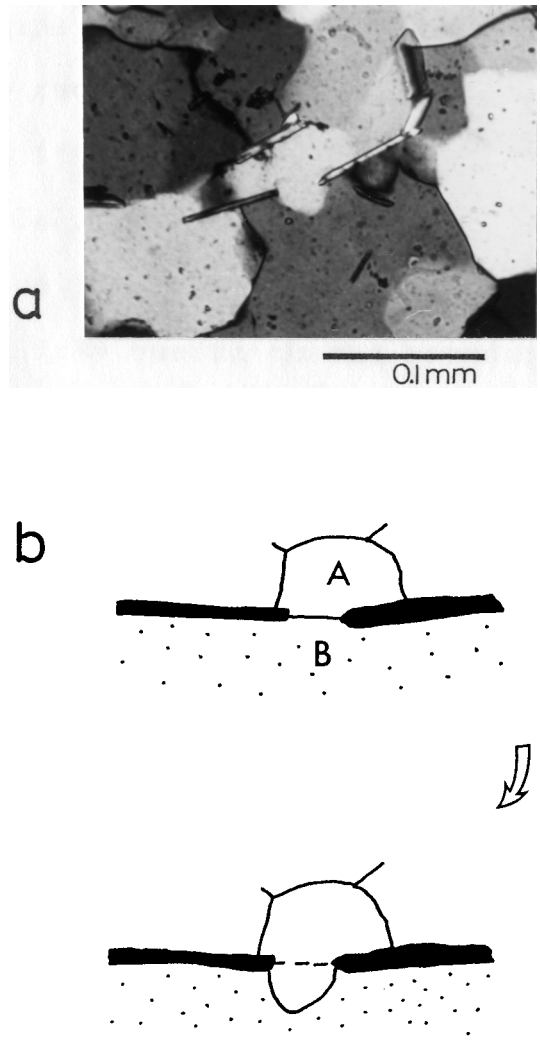

Fig.3.4. a) Photo-micrograph of "window" microstructure.
b) Postulated mode of formation of "window" microstructure. A and B are quartz grains, the black grain is a mica.

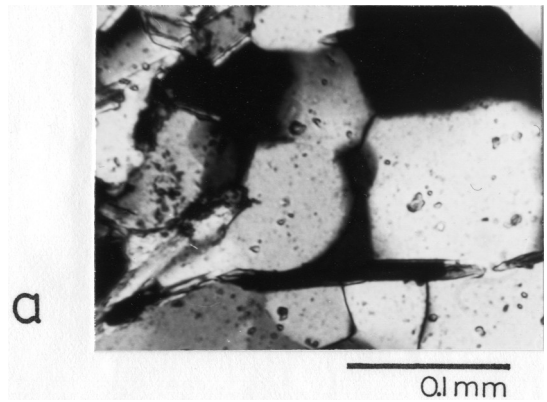

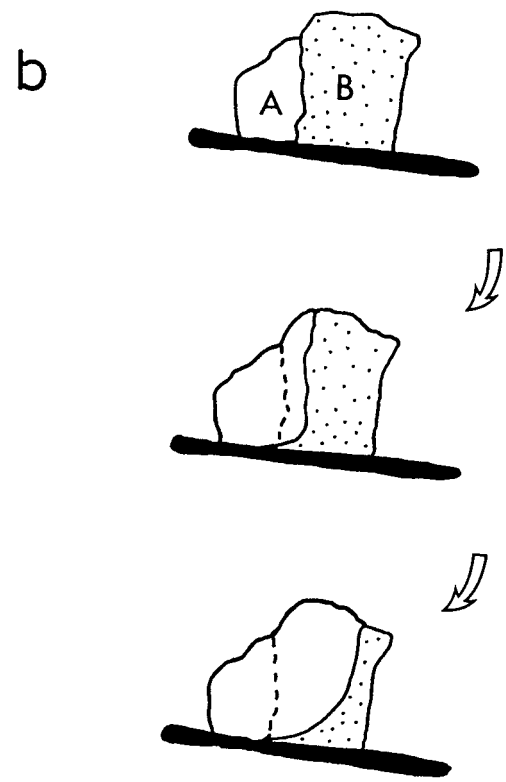

Fig.3.5. a) Photo-micrograph of "dragging" microstructure.
b) Postulated mode of formation of "dragging" microstructure.
A and B are quartz grains, the black grain is a mica.

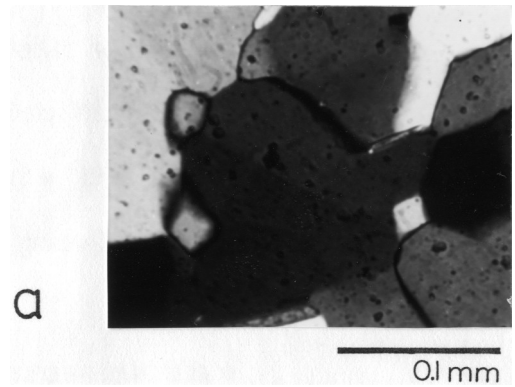

Fig.3.6. a) Photo-micrograph of "left-over grains".
b) Postulated mode of formation of "left-over grains", after Urai (1983). A and B are quartz grains.

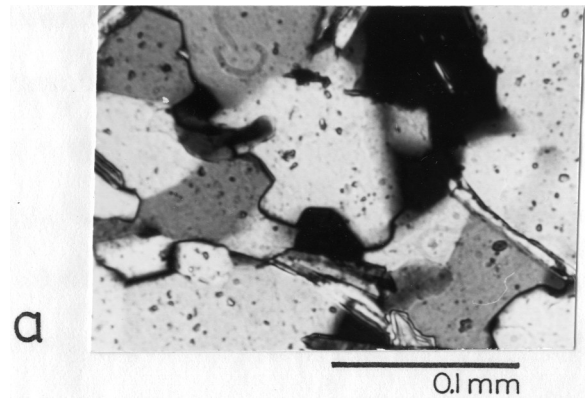

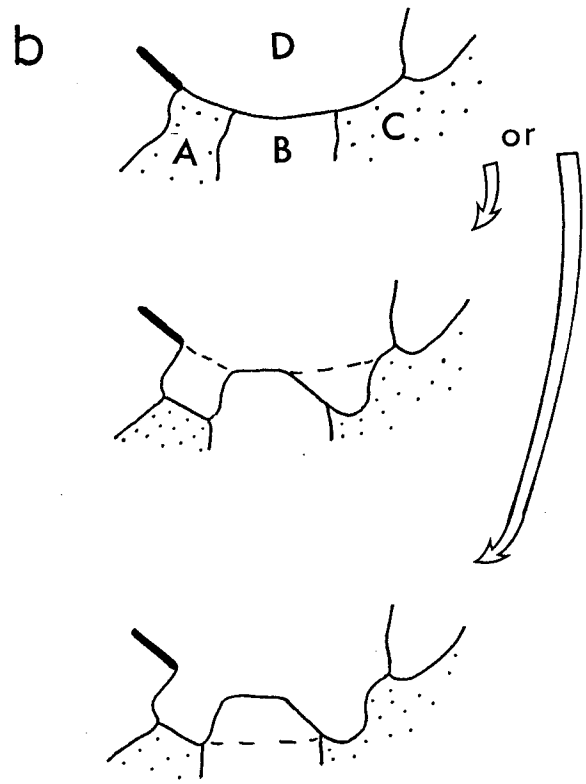

Fig.3.7. a) Photo-micrograph of "castellate" microstructure. b) Alternate postulated modes of formation of "castellate" microstructure. A-D are quartz grains.

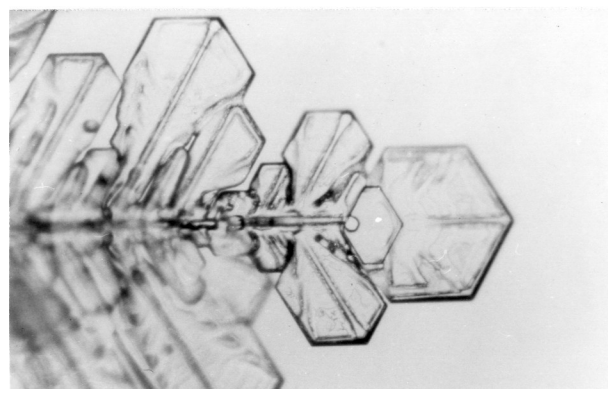

Fig.A.1. Vapour grown dendritic OCP crystal displaying hexagonal crystal forms.

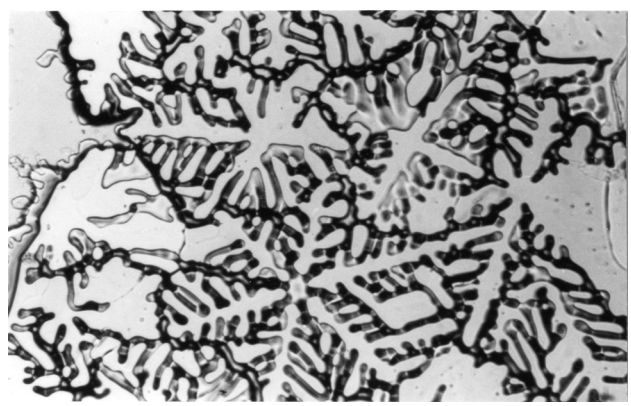

Fig.A.2. Melt grown OCP displaying hexagonal arrays of fluid inclusions.

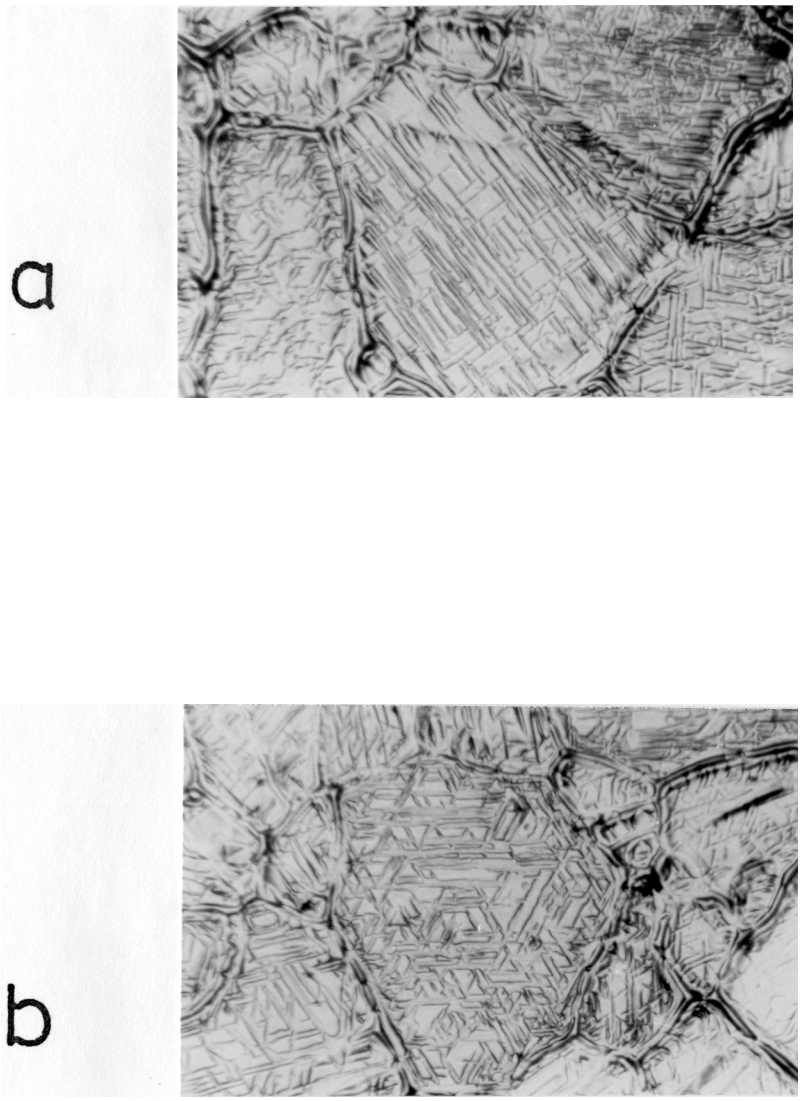

Fig.A.3. Annealed polycrystalline OCP etched in air, displaying crystallographically controlled etch lines. a) central grain has c-axis within plane of photograph, so etch lines are consistent with basal and prism orientations. b) central grain has c-axis perpendicular to plane of photograph, so etch lines are consistant with prism orientations.

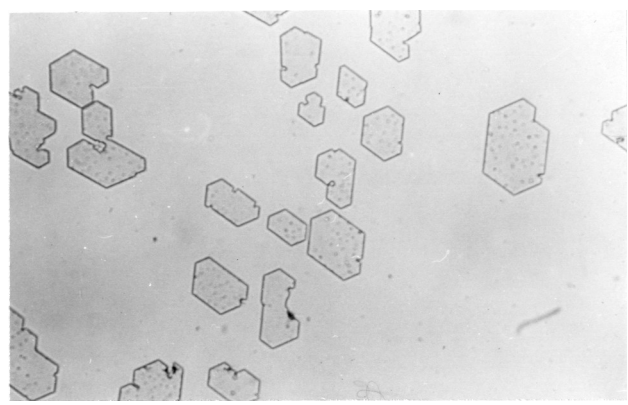

Fig.A.4. Single crystal of OCP grown from the melt, with crystallographically controlled fluid inclusion faces, showing hexagonal forms.

Fig.A.7. Deformation microstructures in OCP. a) Kinks, (or twins) in OCP deformed at high strain rates. b) en echelon deformation features in OCP deformed at high strain rates. c) Fine twins (or kinks) offsetting grain boundary in OCP deformed at high strain rates.

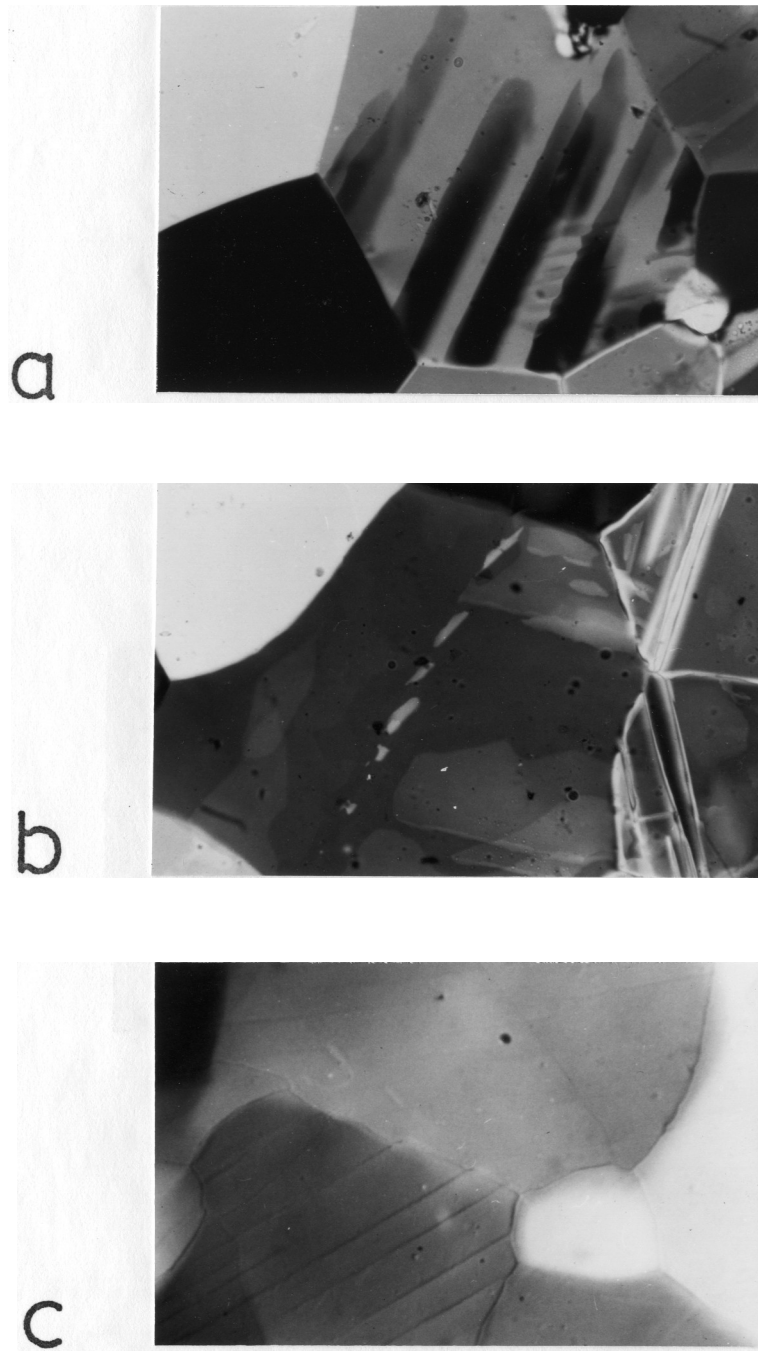

Fig.A.7. Deformation microstructures in OCP. a) Kinks, (or twins) in OCP deformed at high strain rates. b) en echelon deformation features in OCP deformed at high strain rates. c) Fine twins (or kinks) offsetting grain boundary in OCP deformed at high strain rates.

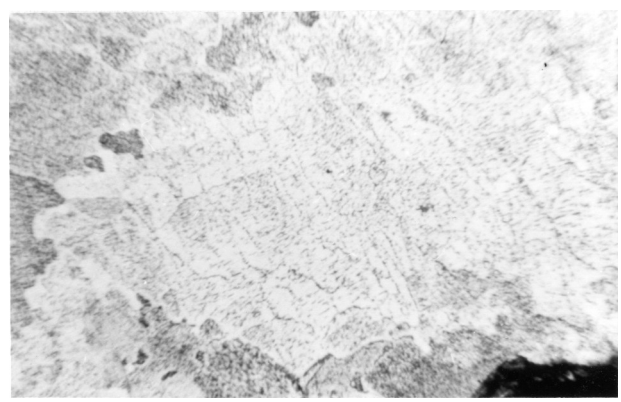

Fig.A.8. Polycrystalline OCP deformed at a strain rate of $5 \times 10^{-5} s^{-1}$, and then etched in air. Etch pits form linear arrays that mark subgrain and grain boundaries.

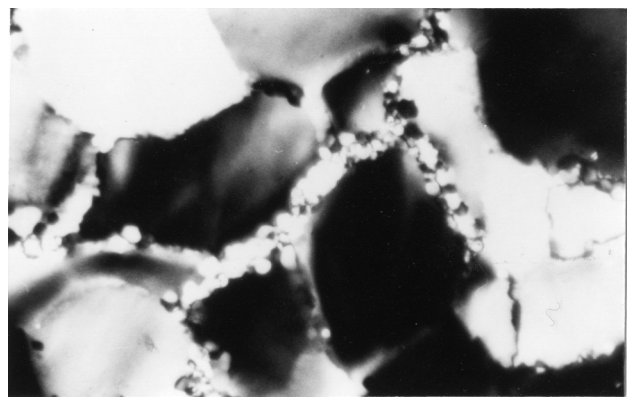

Fig.A.9. Polycrystalline OCP deformed at high strain rates, showing core and mantle structure.